JOURNAL OF Materials CHEMISTRY

Synthesis and structure determination of reduced tantalates, $Li_2LaTa_2O_7$, $Li_2Ca_2Ta_3O_{10}$ and $Na_2Ca_2Ta_3O_{10}$, with a layered perovskite structure

Kenji Toda,[a] Masaki Takahashi,[a] Takashi Teranishi,[a] Zuo-Guang Ye,[a] Mineo Sato[a] and Yukio Hinatsu[b]

[a]*Department of Chemistry and Chemical Engineering, Faculty of Engineering, Niigata University, 8050 Ikarashi 2-nocho, Niigata 950–2181, Japan. E-mail: ktoda@eng.niigata-u.ac.jp*
[b]*Division of Chemistry, Graduate School of Science, Hokkaido University, Sapporo 060–0810, Japan*

Received 8th September 1998, Accepted 21st December 1998

New reduced tantalates, $Li_2LaTa_2O_7$, $Li_2Ca_2Ta_3O_{10}$ and $Na_2Ca_2Ta_3O_{10}$, with a layered perovskite structure have been synthesized by a chemical or an electrochemical intercalation reaction of the alkali metal cations with the parent Dion–Jacobson series compounds. The crystal structures of these compounds were determined by Rietveld analysis of powder X-ray diffraction patterns, and found to be analogous to those of the parent compounds. The intercalation of the lithium ion leads to a large contraction along the stacking direction of perovskite layers because of a higher interlayer charge density. These intercalation compounds are the first example of reduced tantalates with a layered perovskite structure.

Perovskite related compounds have many useful applications such as dielectrics, catalysts and superconductors.[1–6] Their properties are mainly governed by the interaction between transition metals and oxygen. The relationship between crystal structure and transport properties in many low-dimensional materials have attracted much attention. Numerous experimental and theoretical studies have been performed since the discovery of the high temperature superconductor $(La,Ba)_2CuO_4$ with K_2NiF_4-type structure in 1986.[7] The transition metals and oxide ions in a layered perovskite compound form quasi-two-dimensional planes. Such a layered perovskite compound is a suitable system to study two-dimensional physical properties resulting from the transition metal–oxygen plane.

During the last decade a great interest has been taken in the layered perovskites made up of NbO_6 or TiO_6 octahedra, in which the interlayer positions are occupied by alkali metal ions. These compounds exhibit a variety of chemical properties such as ion-exchange and intercalation reactions. There are two series of ion-exchangeable layered perovskites; one is the Ruddlesden–Popper series[8–11] with the general formula $M_2[A_{n-1}B_nO_{3n+1}]$ (M = alkali metal, B = Ti) and the other is the Dion–Jacobson series[12,13] with $M[A_{n-1}B_nO_{3n+1}]$ (M = alkali metal, B = Nb). It is well known that the chemical and electrochemical reduction of the framework B site atoms can occur, accompanied with alkali metal insertion into the interlayer, in the members of the Dion–Jacobson series with partially occupied interlayer site.[14–18] Quite recently, the Hiroshima University group announced that the chemical reduction of the Dion–Jacobson phases could lead to superconductivity at about 6 K.[19] Rousseau *et al.* reported that the electronic structure was strongly dependent on the bond alternation perpendicular to the layer and the off-plane distortion of the equatorial oxygen atoms of MO_6 (M = V and Nb).[20] An important common structural feature for all the series of ion-exchangeable layered perovskite compounds is the presence of extremely short metal–oxygen bonds in the direction of the interlayer alkali metals.

Recently, we disclosed other ion-exchangeable layered perovskite compounds, $RbLaTa_2O_7$ and $RbCa_2Ta_3O_{10}$, constituting new members of the Dion–Jacobson series with $n = 2$ and 3 for the general formula $M[A_{n-1}B_nO_{3n+1}]$.[21] It is expected that a similar reduction process can take place in these new layered perovskite compounds, leading to novel chemical and physical properties. To the best of our knowledge, no reduced tantalates with layered perovskite structure has been found up to now.

Here we report the synthesis and structure determination of new reduced tantalates, $Li_2LaTa_2O_7$, $Li_2Ca_2Ta_3O_{10}$ and $Na_2Ca_2Ta_3O_{10}$, with a layered perovskite structure. The crystal structures of intercalation compounds obtained were determined by Rietveld analysis of powder X-ray diffraction (XRD) patterns. The structural change upon the intercalation is discussed on the basis of the results of the refinement.

Experimental

The starting materials for $RbLaTa_2O_7$ and $RbCa_2Ta_3O_{10}$ were a mixture of rubidium carbonate, lanthanum oxide (or calcium carbonate) and tantalum oxide. An excess amount of rubidium carbonate (50 mol%) was added to compensate for the loss due to the volatilization of the rubidium component. The ground mixtures were pressed into pellets under a pressure of 40 MPa. The pellets were placed in an alumina crucible and then heated at 1373 K. The reaction times were 4 h for $RbLaTa_2O_7$ and 12 h for $RbCa_2Ta_3O_{10}$, respectively.

The lithium and sodium ion-exchanged compounds were prepared by an ion-exchange reaction of the rubidium compound. The ion-exchange was carried out by reacting the parent compounds with molten $LiNO_3$ at 553 K for 24 h and $NaNO_3$ at 673 K for 24 h. After the reaction, the ion-exchanged products were collected, washed with distilled water and air-dried at room temperature. The completion of the ion-exchange reaction was confirmed by XRD and X-ray fluorescence (XRF) analyses.

The chemical lithium insertion was carried out by reacting the sample with a *n*-butyllithium (*n*-BuLi) hexane solution (1.6 M) in a dried glove box filled with argon gas at room temperature for 30 days. The products were stored in the evacuated quartz ampoules because of their high instability in air. The lithium contents in the samples were determined by a back titration of the non-reacted *n*-BuLi with a dilute HCl

solution. The experimental values of the titration were in error by up to 0.03. The electrochemical lithium intercalation was performed using galvanic cells, which were assembled in a glove box filled with argon gas. The electrodes were composed by mixing the ion-exchanged products, acetylene black and polytetrafluoroethylene in a weight ratio of 7 : 2.5 : 1. Lithium plates cut from lithium metal ingots were used for both negative and reference electrodes. The electrolyte was made of 1 M $LiClO_4$ dissolved in a 1 : 1 weight ratio mixture of propylene carbonate and dimethoxyethane. The sodium intercalation was carried out by reacting $NaCa_2Ta_3O_{10}$ with sodium azide NaN_3 in an evacuated quartz tube at 673 K for 20 min. After the decomposition of the azide was completed, the tube was sealed off. The chemical composition of the products was analyzed by XRF analysis.

Powder XRD patterns were recorded on a Rigaku RAD-rA diffractometer equipped with a hand-made attachment for nitrogen gas flow. The data were collected by a step-scanning mode in the 2θ range of 10–100° with a step width 0.02° and a step time 4 s. The powder XRD patterns obtained were indexed with the aid of the computer program CELL.[22] The structure refinement was carried out by the Rietveld method, using the RIETAN94 profile refinement program.[23] The temperature dependence of the magnetic susceptibility was measured for powder samples in quartz ampoules using a Quantum Design MPMS-5S SQUID magnetometer (temperature range: 4.2–300 K; applied field: 50 G). The calibration was made on a blank quartz ampoule under the same conditions.

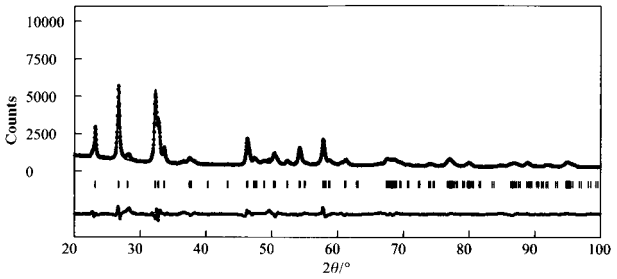

Fig. 1 X-Ray powder pattern fitting for $Li_2LaTa_2O_7$. The calculated and observed patterns are shown on the top by the solid line and the dots, respectively. The vertical marks in the middle show the positions calculated for Bragg reflections. The trace on the bottom is a plot of the difference between the calculated and the observed intensities.

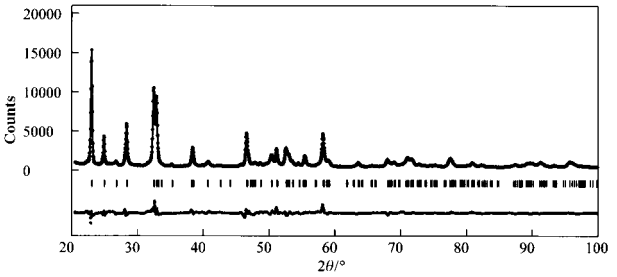

Fig. 2 X-Ray powder pattern fitting for $Li_2Ca_2Ta_3O_{10}$.

Results and discussion

Chemical analyses of the ion-exchanged compounds provided important information on the ordering of the interlayer cations in these layered perovskite compounds. The extrinsic rubidium ions without a pass for the ion transport (rubidium ions in the perovskite layer block of the parent rubidium compounds) does not cause the ion-exchange reaction. If extrinsic rubidium ions exist in the parent compounds, $RbLaTa_2O_7$ and $RbCa_2Ta_3O_{10}$, a rubidium component would be detected after the ion-exchange reaction. The XRF data indicated that there is no detectable amount of the rubidium component after ion-exchange (<0.2 mol%). Therefore, it is clearly indicated that the layered perovskite compounds, $RbLaTa_2O_7$ and $RbCa_2Ta_3O_{10}$, adopt the Dion–Jacobson type structure with completely ordered interlayer cations. Further evidence that the Rb atoms actually occupy the interlayer 1d site in the parent rubidium compounds comes from refinement of site occupancies which confirm that there is no mixing of the two cations (rubidium and lanthanum or rubidium and calcium) between the interlayer and innerlayer A-site. The refined occupancy was found to be approximately equal to the ideal stoichiometry within a standard deviation (<0.04). For example, the refinement of occupancies for the triple layered perovskite, $RbCa_2Ta_3O_{10}$, gives the chemical composition $Rb_{1.00(4)}Ca_{2(0.96(4))}Ta_3O_{10}$. In addition, on crystallographic grounds it is unlikely that the large rubidium cation is distributed in the A site of perovskite block.

After the lithium intercalation reaction of the ion-exchanged samples, $LiLaTa_2O_7$ and $LiCa_2Ta_3O_{10}$, with *n*-BuLi solution, the initially whitish samples turned dark blue with time. As shown in Fig. 1 and 2, the lattice constant along the stacking direction of the perovskite layers becomes smaller after the intercalation process.[21] These phenomena are approximately consistent with the reductive intercalation of the niobate Dion–Jacobson members.[14–18] Clearly, the reaction of parent ion-exchanged samples with *n*-BuLi results in the insertion of additional lithium ions. The samples synthesized by the chemical intercalation are identical to those obtained by electrochemical intercalation, indicating the insertion of one lithium per formula unit. The lithium content determined by the back titration also clearly showed that $Li_2LaTa_2O_7$ and $Li_2Ca_2Ta_3O_{10}$ were formed as the reduced intercalation compounds. Similarly, the white sodium ion-exchanged sample was dark blue after the sodium intercalation reaction. Clearly, the reaction of $NaCa_2Ta_3O_{10}$ with sodium azide results in the insertion of additional sodium ions. The maximum sodium uptake was found to be 1.0. The XRF data indicated that the composition of the product was nearly identical to the nominal one within an experimental error of 0.03. These intercalation compounds can easily be reoxidized when exposed to air at room temperature. The powder XRD patterns of the white reoxidized samples are similar to those of the parent ion-exchanged compounds.

Powder XRD patterns of intercalation compounds are shown in Fig. 1–3. In the double layered perovskite compound $Li_2LaTa_2O_7$, a small discrepancy in the pattern fitting is observed around $2\theta = 28°$. This is due to an unknown impurity formed after the ion-exchange process. The small amount of this impurity does not worsen the reliable factors of the structure refinement and crystallographic data are listed in Table 1. The *R*-factors obtained for the intercalation compounds reasonably converged to acceptable values. The structural models refined for $Li_2LaTa_2O_7$, $Li_2Ca_2Ta_3O_{10}$, $NaCa_2Ta_3O_{10}$ and $Na_2Ca_2Ta_3O_{10}$ are illustrated in Fig. 4 and 5. The crystal structures of lithium intercalation compounds are essentially the same as the corresponding parent ion-exchanged compounds. The adjacent perovskite sheets in the

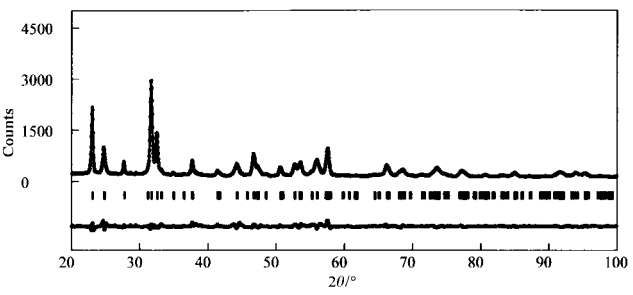

Fig. 3 X-Ray powder pattern fitting for $Na_2Ca_2Ta_3O_{10}$.

Table 1 Crystallographic data for $Li_2LaTa_2O_7$, $Li_2Ca_2Ta_3O_{10}$, $NaCa_2Ta_3O_{10}$ and $Na_2Ca_2Ta_3O_{10}$

Sample	Atom	Site[a]	g[b]	x	y	z	B/nm^2
$Li_2LaTa_2O_7$	Li	4d	1.0	0.0	0.5	0.25	0.05(4)
*I*4/*mmm* (no. 139)	La	2a	1.0	0.0	0.0	0.0	0.008(1)
$a=0.39250(4)$ nm	Ta	4e	1.0	0.0	0.0	0.3872(2)	0.006(1)
$c=1.9089(3)$ nm	O(1)	8g	1.0	0.0	0.5	0.098(2)	0.011(4)
$R_{wp}=7.30\%$	O(2)	4e	1.0	0.0	0.0	0.288(2)	0.011(4)
$R_F=1.23\%$	O(3)	2b	1.0	0.0	0.0	0.5	0.011(4)
$Li_2Ca_2Ta_3O_{10}$	Li	4d	1.0	0.0	0.5	0.25	0.001(1)
*I*4/*mmm* (no. 139)	Ca	4e	1.0	0.0	0.0	0.4204(6)	0.001(1)
$a=0.38927(6)$ nm	Ta(1)	2a	1.0	0.0	0.0	0.0	0.001(1)
$c=2.6591(5)$ nm	Ta(2)	4e	1.0	0.0	0.0	0.1539(1)	0.001(1)
$R_{wp}=9.53\%$	O(1)	4c	1.0	0.0	0.5	0.0	0.001(1)
$R_F=1.67\%$	O(2)	4e	1.0	0.0	0.0	0.074(1)	0.001(1)
	O(3)	8g	1.0	0.0	0.5	0.1381(8)	0.001(1)
	O(4)	4e	1.0	0.0	0.0	0.217(1)	0.001(1)
$NaCa_2Ta_3O_{10}$	Na	4d	0.5	0.0	0.5	0.25	0.004(2)
*I*4/*mmm* (no. 139)	Ca	4e	1.0	0.0	0.0	0.426(1)	0.004(2)
$a=0.38607(3)$ nm	Ta(1)	2a	1.0	0.0	0.0	0.0	0.004(2)
$c=2.9216(2)$ nm	Ta(2)	4e	1.0	0.0	0.0	0.1452(2)	0.004(2)
$R_{wp}=10.62\%$	O(1)	4c	1.0	0.0	0.5	0.0	0.004(2)
$R_F=4.31\%$	O(2)	4e	1.0	0.0	0.0	0.064(2)	0.004(2)
	O(3)	8g	1.0	0.0	0.5	0.135(2)	0.004(2)
	O(4)	4e	1.0	0.0	0.0	0.207(3)	0.004(2)
$Na_2Ca_2Ta_3O_{10}$	Na	4e	1.0	0.0	0.0	0.282(2)	0.001(1)
*I*4/*mmm* (no. 139)	Ca	4e	1.0	0.0	0.0	0.420(1)	0.001(1)
$a=0.38872(5)$ nm	Ta(1)	2a	1.0	0.0	0.0	0.0	0.001(1)
$c=2.8655(4)$ nm	Ta(2)	4e	1.0	0.0	0.0	0.1452(2)	0.001(1)
$R_{wp}=7.85\%$	O(1)	4c	1.0	0.0	0.5	0.0	0.001(1)
$R_F=2.69\%$	O(2)	4e	1.0	0.0	0.0	0.067(3)	0.001(1)
	O(3)	8g	1.0	0.0	0.5	0.122(2)	0.001(1)
	O(4)	4e	1.0	0.0	0.0	0.202(2)	0.001(1)

[a]Multiplicity and Wyckoff notation. [b]Occupancy.

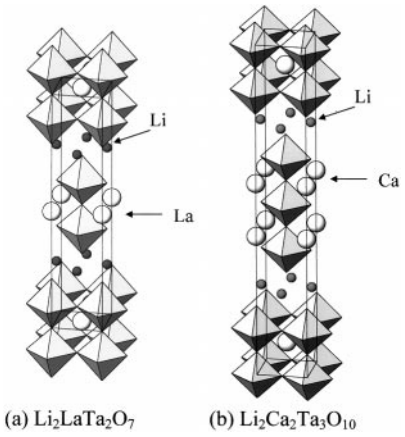

Fig. 4 The structural model for (a) $Li_2LaTa_2O_7$ and (b) $Li_2Ca_2Ta_3O_{10}$.

ion-exchanged and intercalation compounds are stacked with a displacement by 1/2 along the diagonal direction within the perovskite layer plane. The lithium ions in ion-exchanged compounds, $LiLaTa_2O_7$ and $LiCa_2Ta_3O_{10}$, occupy the four-fold sites with a half occupancy.[21] On the other hand, the tetrahedral sites of the intercalation compounds are of full occupancy. The most drastic effect is observed on the c parameter, which shrinks by about 0.135 nm for $Li_2LaTa_2O_7$ and 0.175 nm for $Li_2Ca_2Ta_3O_{10}$, while the a parameter slightly increases. As a result of the large shrinkage, the unit cell volume of both intercalation compounds is contracted. This behavior contrasts somewhat with the results of typical lithium intercalation reactions in transition metal oxides such as MoO_3[24] and Fe_3O_4,[25] where an expansion of the unit cell volume is observed.

The environment around lithium atoms in $LiLaTa_2O_7$ and $Li_2LaTa_2O_7$ is shown in Fig. 6. For the intercalation compound, the LiO_4 tetrahedra are significantly distorted from the ideal tetrahedral arrangement. The coordination of lithium ions approximates to square-planar. The Li–O bond distance [0.209(1) nm] in $Li_2LaTa_2O_7$ is in good agreement with that found for Li–O in other oxides.[26,27] The doubled interlayer charge density of the lithium ion in the intercalation compound leads to a large contraction along the stacking direction of the perovskite layers.

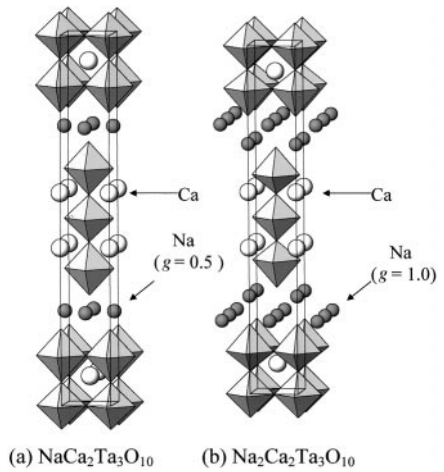

Fig. 5 The structural model for (a) $NaCa_2Ta_3O_{10}$ and (b) $Na_2Ca_2Ta_3O_{10}$.

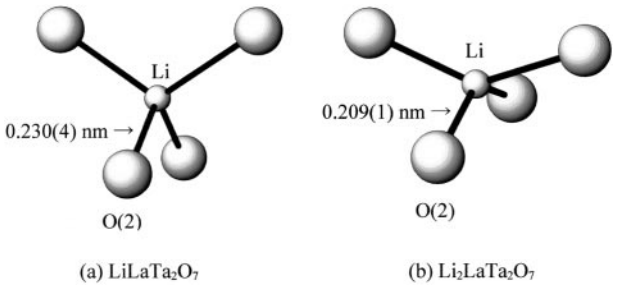

Fig. 6 Environment around the lithium atom in (a) $LiLaTa_2O_7$ and (b) $Li_2LaTa_2O_7$.

Fig. 7 shows the environment of tantalum atoms in $LiLaTa_2O_7$ and $Li_2LaTa_2O_7$. The tantalum atom in the parent compound is fairly displaced from the ideal central position of TaO_6 octahedra. The charge imbalance between lithium and lanthanum ions is compensated by the displacement of the tantalum ions from the center of the regular octahedron toward the lithium ions. The shortest Ta–O bond distance in

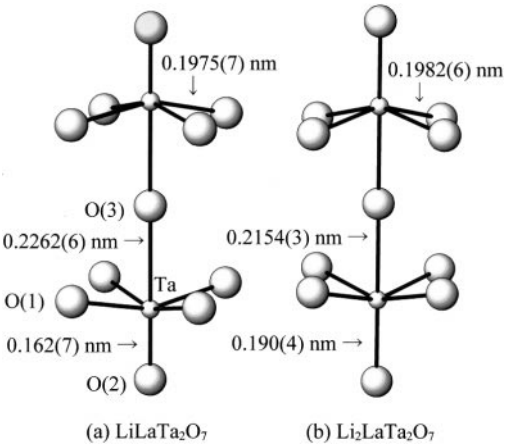

Fig. 7 Environment around the tantalum atom in (a) $LiLaTa_2O_7$ and (b) $Li_2LaTa_2O_7$.

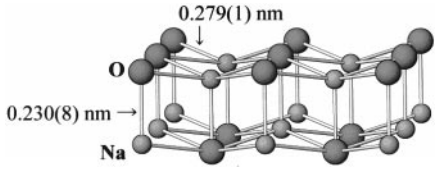

Fig. 8 Environment around the sodium atom in the Ruddlesden–Popper type $Na_2Ca_2Ta_3O_{10}$.

$LiLaTa_2O_7$ is 0.162(7) nm, similar to that of other Dion–Jacobson series members. On the other hand, the distortion of the TaO_6 octahedra is relaxed by the insertion of lithium ions into the intercalation compound. Since the interlayer charge density of $Li_2LaTa_2O_7$ is doubled in comparison with $LiLaTa_2O_7$, the displacement of the tantalum ion in the intercalation compound is smaller than that in the parent compound. However, the octahedron is still somewhat distorted from ideal. The small expansion of *a* parameter observed for the intercalation compound is mainly due to the decrease of the off-plane distortion. The triple layered perovskite, $Li_2Ca_2Ta_3O_{10}$, also shows these structural features.

By contrast, the rock-salt coordination of interlayer sodium ion in the sodium intercalation compound, $Na_2Ca_2Ta_3O_{10}$, is fairly different from the tetrahedral coordination of the parent compound, $NaCa_2Ta_3O_{10}$. The crystal structure of the sodium intercalation compound, $Na_2Ca_2Ta_3O_{10}$, is composed of a triple layered perovskite unit and a rock-salt unit of sodium ion stacked alternately along the *c*-axis. Therefore, this intercalation compound is the first example of a reduced tantalate with a Ruddlesden–Popper type structure.

The environment around sodium atoms in $Na_2Ca_2Ta_3O_{10}$ is shown in Fig. 8. For the intercalation compound, the Na–O planes are significantly distorted from an ideal rock-salt arrangement. The short Na–O bond distance [0.230(8) nm] in $Na_2Ca_2Ta_3O_{10}$ is in good agreement with those found for Na–O in other Ruddlesden–Popper type titanate compounds.[10,28] If the sodium atoms in the intercalation compound have a tetrahedral coordination, the spacing between the adjacent sodium ions would be about 0.275 nm. This interlayer distance is too small to allow the sodium ions to be in a tetrahedral coordination because of strong repulsive force.

Fig. 9 shows the environment of tantalum atoms in $Na_2Ca_2Ta_3O_{10}$. The TaO_6 octahedron located on the inside of the perovskite layers is close to ideal, while those located on the outside of the layer are fairly distorted. The shortest Ta–O bond distance in the intercalation compound is 0.162(6) nm,

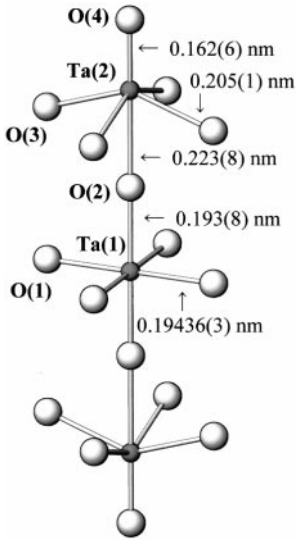

Fig. 9 Environment around the tantalum atom in the Ruddlesden–Popper type $Na_2Ca_2Ta_3O_{10}$.

similar to that of other Dion–Jacobson series members. The Ta–O bonds of the outside octahedra in this compound are classified into three types, *i.e.*, a very short bond [0.162(6) nm] toward the interlayer space, four normal bonds [0.205(1) nm] linked with an equatorial oxygen atom and a long bond [0.223(8) nm] toward the inside of the layer. Rousseau *et al.* reported that the electronic structure was strongly dependent on the bond alternation perpendicular to the layer and the off-plane distortion of the equatorial oxygen atoms.[20] An important common structural feature for all the series of ion-exchangeable layered perovskite compounds is the presence of extremely short metal–oxygen bonds in the direction of the interlayer alkali metals between the perovskite layers.

Given the electrical neutrality in the intercalation compounds, the average formal oxidation states of tantalum in $Li_2LaTa_2O_7$, and $Li_2Ca_2Ta_3O_{10}$, $Na_2Ca_2Ta_3O_{10}$ are +4.5, +4.67 and +4.67, respectively. To the best of our knowledge, these new compounds constitute the first reduced tantalates with the layered perovskite structure to be synthesized. Fujimori *et al.* reported the electronic structure and electron–phonon interaction in transition metal oxides with d^0 configuration and lightly electron doped compounds.[29] The onsite d–d interaction and metal d–oxygen p orbital hybridization are closely related to the atomic number and valence of the transition metal ion. Both strong on-site Coulomb repulsion and electron–phonon interaction are taken into account to study the high-T_c superconductors in many theoretical models. The Ta^{4+} ($5d^1$)–Ta^{5+} ($5d^0$) valences are mutually complementary to Cu^{2+} ($3d^9$)–Cu^{3+} ($3d^8$) with a spin 1/2. Therefore, we are very interested in the relationship between the crystal structure and transport properties in the reduced tantalates.

Finally, we discuss preliminary magnetic susceptibility measurements for the reduced tantalates with the layered perovskite structure. These intercalation compounds show a deep blue color, suggesting a possible delocalization of doped d-electrons. The reduced niobate $Li_xKCa_2Nb_3O_{10}$ is reported to show superconductivity below *ca.* 6 K.[19] This is a second example of a non-cuprate superconductor with the same topology of corner-sharing octahedra as observed in the high temperature superconductor, $La_{2-x}Ba_xCuO_4$.[6,30] The present reduced tantalates show very weak paramagnetic behavior down to 4.2 K and their magnetic susceptibilities are almost constant between 4.2 and 300 K. Fig. 10 shows the temperature dependence of magnetic susceptibility of the intercalation compound, $Na_2Ca_2Ta_3O_{10}$. The temperature-independent term originates from the Pauli paramagnetism, indicating a metallic behavior. These properties are suggestive of those of superconductive hole-doped cuprates. Unfortunately, the precise determination of resistivity is difficult because the intercalation tantalates are highly unstable in air. Our next strategies for searching new non-cuprate superconductors would consist in a complete control of the doping d-electron concentration and the preparation of solid solutions between the two Dion–Jacobson series, $M_{1+x}[A_{n-1}Nb_nO_{3n+1}]$ and

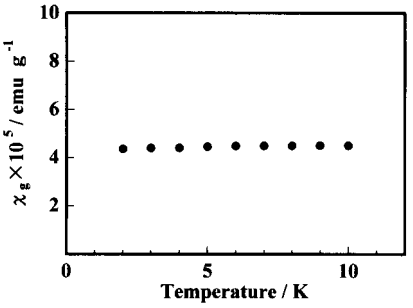

Fig. 10 Temperature dependence of the magnetic susceptibility for the Ruddlesden–Popper type $Na_2Ca_2Ta_3O_{10}$.

$M_{1+x}[A_{n-1}Ta_nO_{3n+1}]$. These studies are in progress and the results will be reported in forthcoming papers.

Acknowledgments

This work was supported by the 'Research for the Future, Preparation and Application of Newly Designed Solid Electrolytes (JSPS RFTF96P00102)' program from the Japan Society for the Promotion of Science (JSPS).

The authors gratefully thank Mr K. Uematsu for his help in preparation of samples. We are indebted to Mr T. Iwafune and Dr M. Wakeshima for their help in data collection of X-ray powder diffraction and magnetic susceptibility measurements, respectively.

References

1 J. F. Schooley, W. R. Hosler and M. L. Cohen, *Phys. Rev. Lett.*, 1964, **12**, 474.
2 J. M. Bolts and M. S. Wrighton, *J. Phys. Chem.*, 1976, **80**, 2641.
3 R. J. D. Tilley, *J. Solid State Chem.*, 1977, **21**, 293.
4 H. H. Kung, H. S. Jarett, A. W. Sleight and A. Feretti, *J. Appl. Phys.*, 1977, **48**, 2463.
5 K. Wakino, K. Minai and H. Tamura, *J. Am. Ceram. Soc.*, 1984, **67**, 278.
6 K. A. Muller and W. Berlinger, *Phys. Rev. B*, 1986, **34**, 6130.
7 J. D. Bednorz and K. A. Muller, *Z. Phys. B*, 1986, **64**, 189.
8 M. Gondrand and J. C. Joubert, *Rev. Chim. Miner.*, 1987, **24**, 33.
9 J. Gopalakrishnan and V. Bhat, *Inorg. Chem.*, 1987, **26**, 4299.
10 K. Toda, Y. Kameo, M. Fujimoto and M. Sato, *J. Ceram. Soc. Jpn.*, 1994, **102**, 737.
11 K. Toda, S. Kurita and M. Sato, *Solid State Ionics*, 1995, **81**, 267.
12 M. Dion, M. Ganne and M. Tournoux, *Mater. Res. Bull.*, 1981, **16**, 1429.
13 A. J. Jacobson, J. T. Lewandowski and J. W. Johnson, *J. Less Common Met.*, 1986, **116**, 137.
14 R. Jones and W. R. McKinnon, *Solid State Ionics*, 1991, **45**, 173.
15 P. Gomez-Romero, M. R. Palacin, N. Casan and A. Fuertes, *Solid State Ionics*, 1993, **63–65**, 424.
16 A. R. Armstrong and P. A. Anderson, *Inorg. Chem.*, 1994, **33**, 4366.
17 M. Sato, T. Jin and H. Ueda, *Chem. Lett.*, 1994, 161.
18 C. Bohnke, O. Bohnke and J. L. Fourquet, *J. Electrochem. Soc.*, 1997, **144**, 1151.
19 H. Fukuoka, T. Isami and S. Yamanaka, *Chem. Lett.*, 1997, 703.
20 R. Rousseau, M. R. Palacin, P. Gomez-Romero and E. Canadell, *Inorg. Chem.*, 1996, **35**, 1179.
21 K. Toda and M. Sato, *J. Mater. Chem.*, 1996, **6**, 1067.
22 Y. Takaki, T. Taniguchi, H. Yamaguchi and T. Ogura, *J. Ceram. Soc. Jpn. Int. Ed.*, 1987, **95**, 565.
23 Y.-I. Kim and F. Izumi, *J. Ceram. Soc. Jpn.*, 1994, **102**, 401.
24 M. S. Whittingham, *Prog. Solid State Chem.*, 1978, **12**, 41.
25 M. S. Islam and C. R. A. Catlow, *J. Solid State Chem.*, 1988, **77**, 180.
26 R. D. Shannon, *Acta Crystallogr., Sect. A*, 1976, **32**, 751.
27 N. K. McGuire and M. O'Keeffe, *J. Solid State Chem.*, 1984, **54**, 49.
28 K. Toda, Y. Kameo, S. Kurita and M. Sato, *J. Alloys Compd*, 1996, **234**, 19.
29 A. Fujimori, A. E. Bocquet, K. Morikawa, K. Kobayashi, T. Saitoh, Y. Tokura, I. Hase and M. Onoda, *J. Phys. Chem. Solids*, 1996, **57**, 1379.
30 Y. Maeno, H. Hashimoto, K. Yoshida, S. Nishizaki, T. Fujita, J. G. Bednorz and F. Lichtenberg, *Nature*, 1994, **372**, 532.

Paper 8/07038E